수의학석사 학위논문

Tolfenamic acid inhibits tumor cell growth by YAP and TAZ degradation

톨페남산(Tolfenamic acid)에 의한 YAP 및 TAZ 단백질 분해와 암세포 성장 억제 효과

2023년 2월

서울대학교 대학원

수의학과 수의생명과학전공
(수의분자세포생물학)

김 일 주

Master's Thesis of Veterinary Medicine

Tolfenamic acid inhibits tumor cell growth by YAP and TAZ degradation

톨페남산(Tolfenamic acid)에 의한 YAP 및 TAZ 단백질 분해와 암세포 성장 억제 효과

February 2023

Major in Veterinary Biomedical Sciences
Department of Veterinary Medicine
Graduate School of Seoul National University

KIM Ilju

Tolfenamic acid inhibits tumor cell growth by YAP and TAZ degradation

톨페남산(Tolfenamic acid)에 의한 YAP 및 TAZ 단백질 분해와 암세포 성장 억제 효과

지도교수 백 승 준

이 논문을 수의학석사 학위논문으로 제출함

2022년 11월

서울대학교 대학원

수의학과 수의생명과학전공

(수의분자세포생물학)

김 일 주

김일주의 수의학석사 학위논문을 인준함

2023년 1월

위 원 장	조 제 열	(인)
부위원장	백 승 준	(인)
위 원	이 소 영	(인)

Abstract

Tolfenamic acid inhibits tumor cell growth by YAP and TAZ degradation

KIM Ilju

Major in Veterinary Biomedical Sciences

Department of Veterinary Medicine

Graduate School of Seoul National University

Hippo pathway is a signaling pathway that plays an important role in cell proliferation and cancer metastasis. Several diseases such as cancer are related to the improper regulation of this pathway. Overactivation of YAP and TAZ proteins, the main effectors of Hippo pathway, accelerates cell proliferation, migration, and invasion during tumorigenesis. Tolfenamic acid (TA) is a non-steroidal anti-inflammatory drug (NSAID) that exhibits anti-cancer activity against various types of cancer. In this study, it was observed that TA decreased YAP and TAZ protein level in cancer cells. TA increased the YAP and TAZ phosphorylation, leading to YAP/TAZ degradation in the cytoplasm and nucleus. TA predominantly affected phosphodegron sites in TAZ, causing TAZ to enter the ubiquitination pathway. Proteins that affect YAP/TAZ protein level, such as NAG-

1 and several YAP/TAZ E3 ligases, were not involved in TA-mediated YAP/TAZ degradation. In summary, our results indicate that TA affects phosphodegron sites on TAZ, which demonstrates a novel effect of TA in tumorigenesis.

Keywords: Hippo pathway, YAP, TAZ, NAG-1, 14-3-3, anti-cancer

Student Number: 2021-24740

Table of Contents

List of Figures

List of Tables

1. Introduction

Cancer-related mortality is currently the second most common cause of death in the US (Ahmad & Anderson, 2021)(Table 1), despite considerable advancements in cancer research and improvements in therapeutics. Recently, the field of precision medicine has become an area of interest, in which patients are treated with personalized drugs; however, the development of such therapies is limited by a lack of comprehensive understanding of cancer. One field of precision medicine involves targeted therapies, in which specific pathways and proteins contributing to tumor generation are identified and targeted.

Table 1. The number of deaths for leading causes of death, US, 2015-2020. (Ahmad & Anderson, 2021)

Table. Number of Deaths for Leading Causes of Death, US, 2015-2020[a]

	No. of deaths by year					
Cause of death	2015	2016	2017	2018	2019	2020
Total deaths	2 712 630	2 744 248	2 813 503	2 839 205	2 854 838	3 358 814
Heart disease	633 842	635 260	647 457	655 381	659 041	690 882
Cancer	595 930	598 038	599 108	599 274	599 601	598 932
COVID-19[b]						345 323
Unintentional injuries	146 571	161 374	169 936	167 127	173 040	192 176
Stroke	140 323	142 142	146 383	147 810	150 005	159 050
Chronic lower respiratory diseases	155 041	154 596	160 201	159 486	156 979	151 637
Alzheimer disease	110 561	116 103	121 404	122 019	121 499	133 382
Diabetes	79 535	80 058	83 564	84 946	87 647	101 106
Influenza and pneumonia	57 062	51 537	55 672	59 120	49 783	53 495
Kidney disease	49 959	50 046	50 633	51 386	51 565	52 260
Suicide	44 193	44 965	47 173	48 344	47 511	44 834

[a] Leading causes are classified according to underlying cause and presented according to the number of deaths among US residents. For more information, see the article by Heron.[4] Source: National Center for Health Statistics. National Vital Statistics System: mortality statistics (http://www.cdc.gov/nchs/deaths.htm). Data for 2015-2019 are final; data for 2020 are provisional.

[b] Deaths with confirmed or presumed COVID-19, coded to *International Statistical Classification of Diseases and Related Health Problems, Tenth Revision* code U07.1 as the underlying cause of death.

The Salvador-Warts-Hippo pathway (Hippo pathway) is an evolutionally conserved pathway that regulates cell fate, homeostasis, tissue growth, and tissue regeneration. It was first discovered in *Drosophila melanogaster* in 2002 and has emerged as an important tumor suppressor signaling pathway (Calses, Crawford, Lill, & Dey, 2019; Sebio & Lenz, 2015)(Figure 1). The core components of the mammalian Hippo pathway are MST1/2, large tumor suppressor 1/2 (LATS1/2), Yes-associated protein (YAP), and transcriptional coactivator with PDZ-binding motif (TAZ, also known as WWTR1)(Figure 2). YAP and TAZ, the main effectors of Hippo pathway, are regulated by the upstream kinases MST1/2 and LATS1/2 and control tumorigenesis (Chen et al., 2019; Sebio & Lenz, 2015; Zanconato, Cordenonsi, & Piccolo, 2016). The activity of YAP/TAZ is important in tumor development as they regulate tissue homeostasis and alters cellular state, and their activity is constitutively upregulated in cancer tissue (Figure 3). The other upstream proteins also affect YAP/TAZ activity, including mammalian Salvador homolog 1 (SAV1), and MOB Kinase Activator 1 (MOB1) (Juan & Hong, 2016; Kim et al., 2017). When Hippo pathway is off, effector proteins YAP and TAZ move into the nucleus and bind to the transcriptional enhanced associate domain (TEAD) transcriptional factor, thereby enhancing the expression of TEAD-dependent genes, such as connective tissue growth factor (CTGF), Cyr61, and

Vimentin (Song et al., 2019; Yu, Zhao, & Guan, 2015) (Figure 4, left panel). On the other hand, if Hippo pathway is on, YAP/TAZ are phosphorylated by LATS1/2 on multiple phosphorylation sites, resulting in subsequent cytoplasmic retention by 14-3-3 protein binding or proteasomal degradation by ubiquitination (Figure 4, right panel). Vestigial-like family member 4 (VGLL4), which competes with YAP/TAZ for TEAD interaction, binds with TEAD when Hippo pathway is off, resulting in TEAD target gene repression. YAP/TAZ are also phosphorylated in pathways associated with cell stress and G-protein coupled receptor signaling (Piccolo, Cordenonsi, & Dupont, 2013; Piccolo, Dupont, & Cordenonsi, 2014), or directly phosphorylated by AKT, GSK3β, and AMPK (Basu, Totty, Irwin, Sudol, & Downward, 2003; Huang et al., 2012; Mo et al., 2015; Piccolo et al., 2014; B. Zhang et al., 2017), upon which they sustain or get degraded in the cytoplasm, inhibiting the TEAD activity (Piccolo et al., 2014; Sebio & Lenz, 2015). YAP and TAZ have similar regulatory domains including TEAD binding site and WW domain. Both YAP and TAZ have specific phosphorylation sites for 14-3-3 protein and also have 'phosphodegron' site that makes protein get ubiquitinated by protein-specific E3 ubiquitin ligase such as $SCF^{\beta-TrCP}$, leading to proteasomal degradation (Chen et al., 2019) (Figure 5). Furthermore, TAZ can be phosphorylated at several serine residues, including serine 58, 62, 89, 311, and 314 (Huang et

al., 2012; Varelas, 2014), followed by its degradation in the cytoplasm in a ubiquitin-dependent manner (Piccolo et al., 2014; Piersma, Bank, & Boersema, 2015; Varelas, 2014). Whereas YAP phosphorylation related to degradation occurs at serine 381, 397 (Varelas, 2014). In human tumors, YAP/TAZ proteins are highly activated, which contributes to cancer initiation, progression, and metastasis. They are also involved in drug resistance in colon, lung, stomach, breast, ovarian, uterine, prostate, liver, and bone cancer (Zanconato et al., 2016).

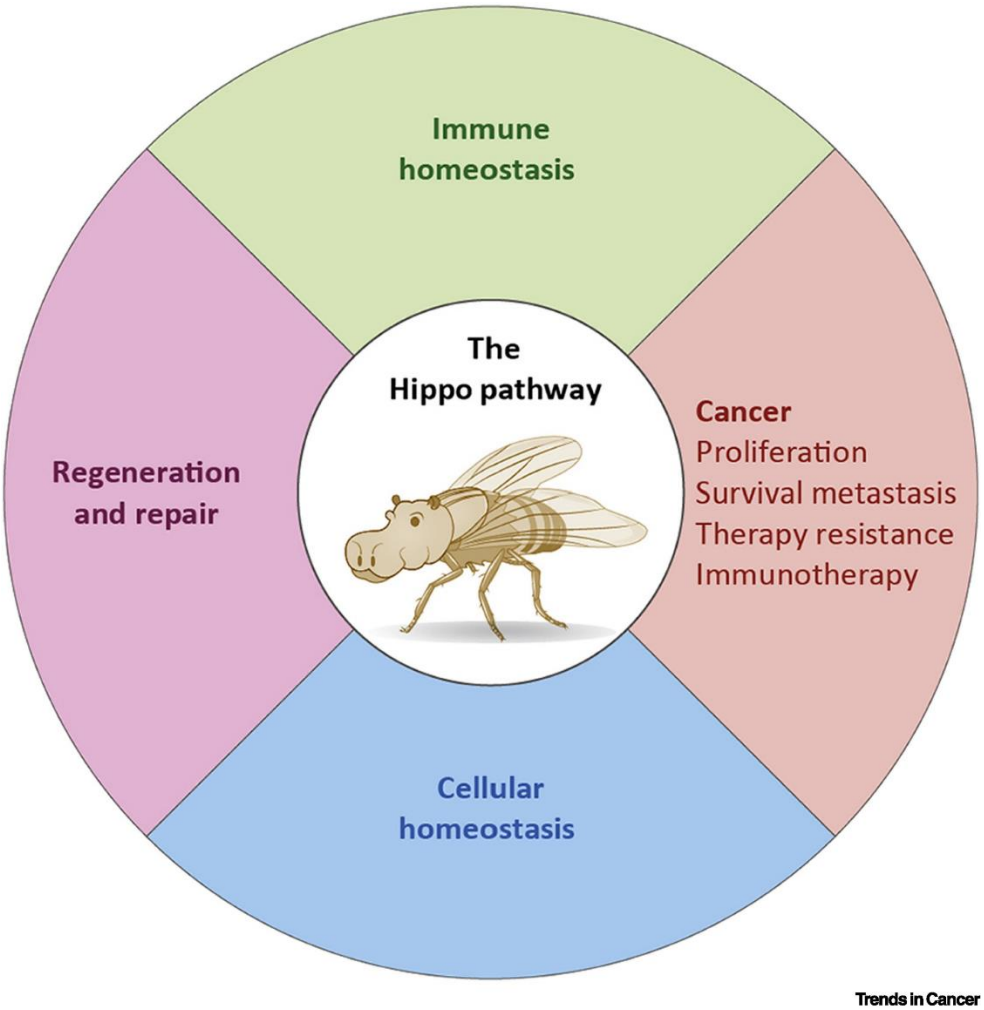

Figure 1. The Functions of Hippo pathway. (Calses, Crawford, Lill, & Dey, 2019)

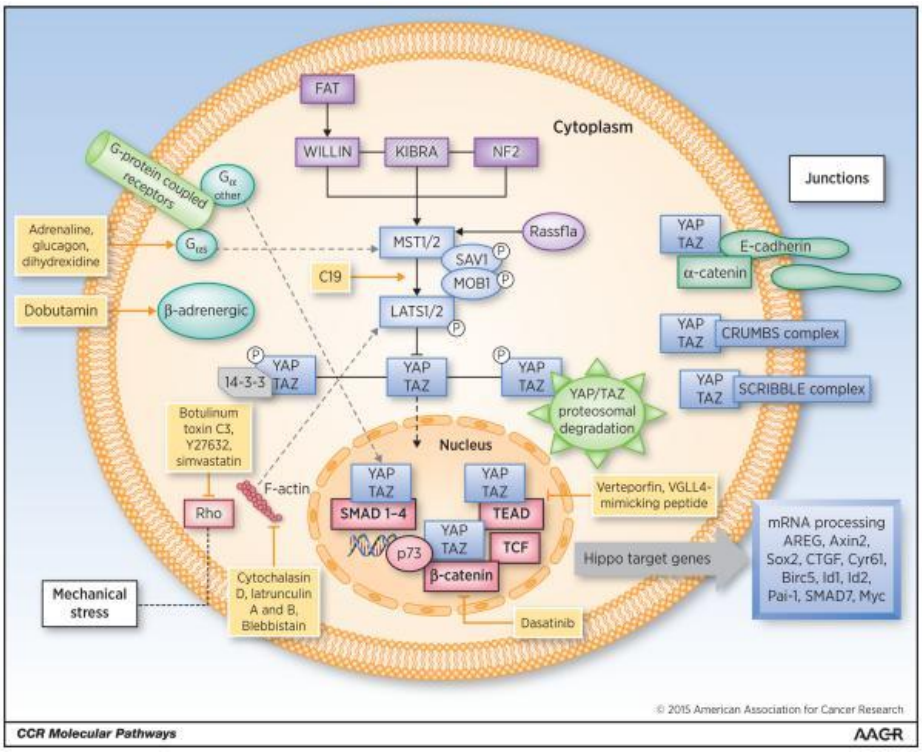

Figure 2. Hippo signaling pathway and main regulators. (Sebio & Lenz, 2015)

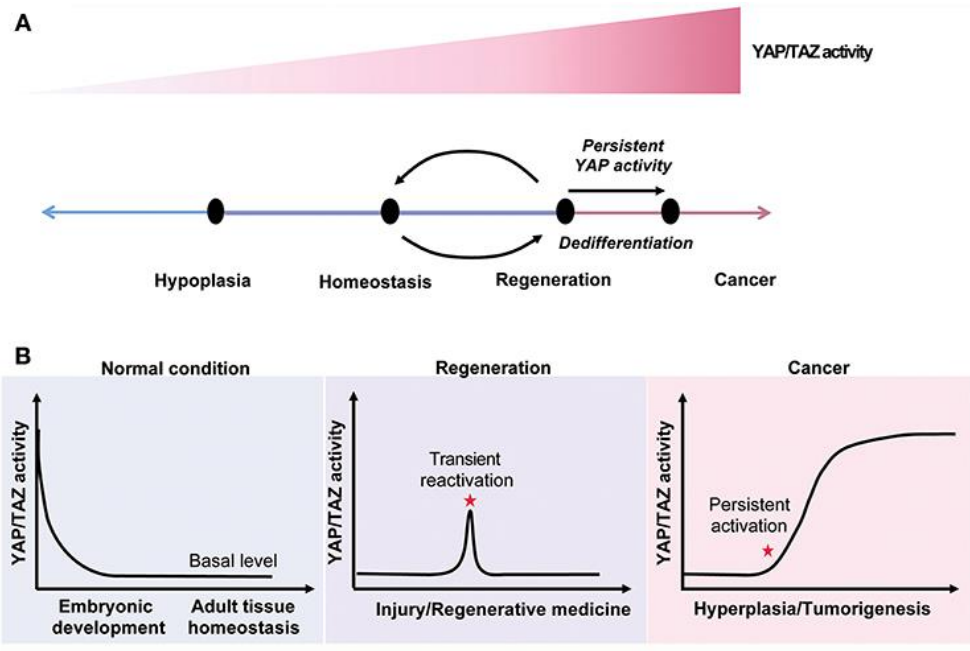

Figure 3. The Hippo signaling pathway in tissue homeostasis, regeneration, and cancer. (Chen *et al.*, 2019)

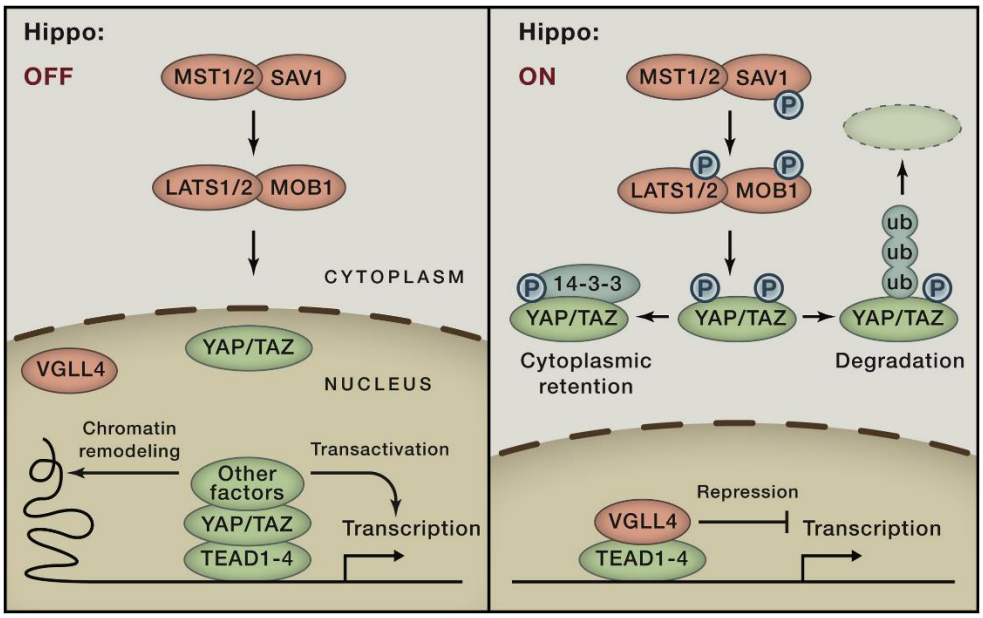

Figure 4. Inhibition of YAP/TAZ transcriptional coactivators by LATS1/2. (Yu, Zhao, & Guan, 2015)

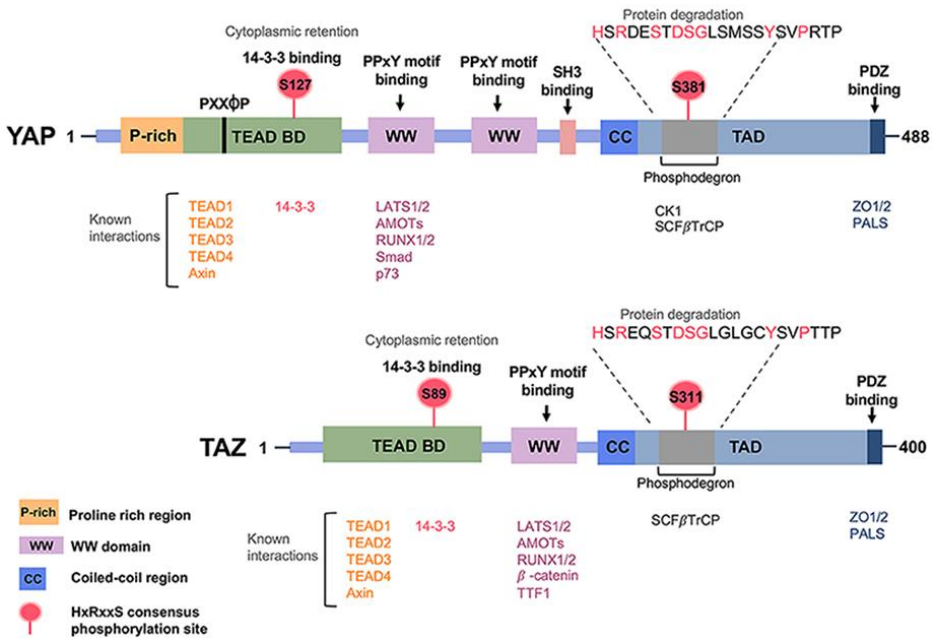

Figure 5. Regulatory domains of the Hippo pathway effector proteins YAP and TAZ. (Chen *et al.*, 2019)

Tolfenamic acid (TA) is a traditional non-steroidal anti-inflammatory drug (NSAID) that is widely used for migraine treatment (P. E. Hansen, 1994). TA was first reported to exhibit anti-cancer activity by suppressing tumorigenesis and metastasis in a pancreatic cancer model (Maen Abdelrahim, Baker, Abbruzzese, & Safe, 2006). The anti-cancer activity of TA was associated with decreased expression of the Sp1 transcription factor and vascular endothelial growth factor (VEGF) (Maen Abdelrahim et al., 2006; M. Abdelrahim et al., 2007). Subsequently, researchers found that TA significantly suppressed the growth of human colorectal cancer cells and enhanced apoptosis in a COX-independent manner (Lee et al., 2008; Lee, Bahn, Whitlock, & Baek, 2010; X. Zhang, Min, Liggett, & Baek, 2013). Concerning toxicity, TA exhibits fewer upper gastrointestinal side effects than other NSAIDs (S. H. Hansen & Pedersen, 1986), which further suggests the potential use of TA as an anti-cancer drug for colorectal cancer. Without understanding the underlying biological mechanisms of TA, clinical prevention or treatment studies are less valuable. Therefore, it is necessary to determine the mechanism of action responsible for the anti-cancer effects of TA and pre-clinical studies using animal models that will yield data to support clinical trials.

In this study, the effects of TA on the Hippo pathway were examined and found that TA treatment appears to increase YAP/TAZ

ubiquitination by E3 ubiquitin ligase. This is the first study to demonstrate that TA increases YAP/TAZ degradation, resulting in tumor growth suppression and anti-cancer activity.

2. Materials and Methods

2.1. Cell lines and tumor specimens

The human SW480, HCT116, and U2OS cell lines were purchased from the American Type Culture Collection (Manassas, VA, USA) and the LoVo cell line was purchased from the Korean Cell Line Bank (Seoul, Korea). BCPAP cells were obtained from Dr. Gary Clayman (MD Anderson, Houston, TX, USA). The cells were tested by the ATCC for post-freeze viability, growth properties, morphology, mycoplasma contamination, species determination (cytochrome c oxidase I assay and short tandem repeat analysis), sterility, and human pathogenic viruses. The cell lines were immediately resuscitated once received and frozen in aliquots of liquid nitrogen. Cells were cultured and maintained in Roswell Park Memorial Institute (RPMI) 1640 medium (Welgene, Gyeongsan, Korea) supplemented with 10% fetal bovine serum (FBS; Life Technologies Corporation, Grand Island, NY, USA) and 1% penicillin-streptomycin (Life Technologies). All the cells were maintained in a humidified incubator with 5% CO_2 at 37°C. For the *in vitro* experiments, 0.1% dimethyl sulfoxide (DMSO; Biosesang, Seongnam, Korea) was used as a control. The human tissue samples used in this study included human thyroid tumor tissues and matched adjacent normal tissues. All the tissue samples were obtained from the National Cancer Center

(Goyang, Korea) and stored at −80°C. This study was approved by the Institutional Review Board of the National Cancer Center (NCC-1810150).

2.2. Reagents and antibodies

TA was purchased from Cayman Chemical (Ann Arbor, MI, USA). Cycloheximide and epoxomicin were purchased from Sigma-Aldrich (St. Louis, MO, USA). MG132 was purchased from MedChemExpress (Monmouth Junction, NJ, USA). Antibodies against YAP/TAZ (#8418; Cell Signaling Technology, Danvers, MA, USA), YAP (sc-101199; Santa Cruz Biotechnology, Dallas, TX, USA), TAZ (#70148; Cell Signaling Technology), Flag (F1804; Sigma-Aldrich), HA (#26183; Thermo Fisher Scientific, Waltham, MA, USA), Pan 14-3-3 (sc-1657; Santa Cruz Biotechnology), V5 (#R960-25; Thermo Fisher Scientific), β-TrCP (#4394; Cell Signaling Technology), Fbxw7 (ab109617; Abcam, Cambridge, UK), USP9X (#5751; Cell Signaling Technology), USP10 (#8501; Cell Signaling Technology), GAPDH (sc-47724; Santa Cruz Biotechnology), β-actin (sc-47778; Santa Cruz Biotechnology), Lamin A/C (sc-376248; Santa Cruz Biotechnology), and α-tubulin (sc-8035; Santa Cruz Biotechnology) were used for western blotting analysis. The NAG-1 antibody has been previously described (Baek, Kim, Nixon, Wilson, & Eling, 2001). The anti-flag antibodies, DYKDDDDK Tag Polyclonal

Antibody (#PA1-984B; Thermo Fisher Scientific) and DDDDK-Tag Rabbit mAb (#AE092; ABclonal, Wuhan, Hubei, China), were used for immunoprecipitation, whereas antibodies against flag (F1804; Sigma-Aldrich) and goat anti-mouse IgG conjugated with FITC (F2761; Thermo Fisher Scientific) were used for immunocytochemistry.

2.3. Cell viability assay

The CellTiter 96 AQ_{ueous} One solution (Promega, Madison, WI, USA) was used to measure relative cell viability according to the manufacturer's protocol. The cells were plated in complete culture media in 96-well culture plates and grown overnight. Then, the cells were treated with various concentrations of TA in complete media and incubated for 0, 24, and 48 h. After removing the media, a mixture of 100 μl of complete media and 20 μl of the One solution reagent was added to each well and incubated for 1 h at 37°C in a 5% CO_2 incubator. Cell viability (absorbance) was measured at 492 nm using a microplate reader (Multiskan™ FC Microplate Photometer, Thermo Scientific, Waltham, MA, USA).

2.4. Plasmid and siRNA transfection

Plasmid transfections were performed using the PolyJet™ In Vitro

DNA Transfection Reagent (SignaGen Laboratories, Frederick, MD, USA), and small interfering RNA (siRNA) transfections were performed using the PepMute™ siRNA Transfection Reagent (SignaGen Laboratories) according to the manufacturer's instructions. Control siRNA-A (sc-37007), siNAG-1 (sc-39798), and siTAZ (sc-38568) were purchased from Santa Cruz Biotechnology. The constructs, pcDNA3.1-V5-NAG-1 WT, pcDNA3.1-V5-NAG-1 RXXR mutant (R193A), pcDNA3.1-V5-NAG-1 ⊿NLS (⊿211-218), and pcDNA3.1-V5-NAG-1 ⊿NES (⊿14-29) were previously described (Min et al., 2016). The p2xflag-YAP, pHA-Ub, pHA-14-3-3β, and p8xGTIIC-luciferase (synthetic TEAD luciferase reporter) constructs were purchased from Addgene (Watertown, MA, USA), whereas p3xflag-TAZ WT was provided by Dr. Kun-Liang Guan (University of California, San Diego, USA). The mutant constructs p3xflag-TAZ S58/62A, p3xflag-TAZ S66A, p3xflag-TAZ S89/90A, p3xflag-TAZ S311/314A, and p3xflag-TAZ S66/89/311/314A were generated using the QuikChange II Site-Directed Mutagenesis Kit (Agilent Technologies, Santa Clara, CA, USA) according to the manufacturer's instructions.

2.5. Dual-Luciferase® Reporter assay

HCT116 cells were transfected with the YAP/TAZ-responsive

TEAD luciferase reporter plasmid p8xGTIIC-luciferase, Renilla luciferase control reporter pRL-null (Promega), with pcDNA3.1 Neo (empty vector) or flag-YAP or flag-TAZ using the PolyJet™ In Vitro DNA Transfection Reagent. Cells were treated with TA and harvested with passive lysis buffer 24 h after treatment. The cell lysates were mixed with luciferase assay reagent II and firefly luciferase light emission was measured using the Dual-Luciferase® Reporter Assay kit (Promega). Renilla luciferase activity was measured to assess firefly luciferase activity.

2.6. RNA extraction and quantitative real-time PCR

Total RNA was isolated with the Invitrogen™ TRIzol™ Reagent (Thermo Fisher Scientific, Rockford, IL, USA) and reverse-transcribed into cDNA using the Verso cDNA Synthesis Kit (Thermo Fisher Scientific). Quantitative real-time PCR reactions were set up with 2X PowerUp™ SYBR™ Green Master Mix (Thermo Fisher Scientific) following the manufacturer's instructions. For quantitation of mRNA expression, the $2^{-\Delta\Delta Ct}$ method was used. Glyceraldehyde 3-phosphate dehydrogenase (GAPDH) was used for normalization. The sequence for each primer was as follows:

hGAPDH F: 5' - GAAGGTGAAGGTCGGAGTCA -3'

hGAPDH R: 5' - GACAAGCTTCCCGTTCTCAG -3'

hNAG-1 F: 5' - GGTGTCGCTCCAGACCTATG -3'

hNAG-1 R: 5' - GGAACCTTGAGCCCATTCCA -3'

hYAP F: 5' - CTCGAACCCCAGATGACTTC -3'

hYAP R: 5' - CCAGGAATGGCTTCAAGGTA -3'

hTAZ F: 5' - GAGGACTTCCTCAGCAATGTGG -3'

hTAZ R: 5' - CGTTTGTTCCTGGAAGACAGTCA -3'

hTEAD1 F: 5' - CCTGGCTATCTATCCACCATGTG -3'

hTEAD1 R: 5' - TTCTGGTCCTCGTCTTGCCTGT -3'

hCTGF F: 5' - CTTGCGAAGCTGACCTGGAAGA -3'

hCTGF R: 5' - CCGTCGGTACATACTCCACAGA -3'

2.7. Western blotting analysis and Phos-tag^{TM} gel preparation

Total protein extracts were isolated using radioimmunoprecipitation assay (RIPA) Lysis Buffer (BIOMAX, Seoul, South Korea) supplemented with 0.5% Universal Protease Inhibitor Cocktail (BIOMAX) and 1 mM NaF and 1 mM Na_3VO_4. The protein concentration of the lysates was assayed using the bicinchoninic acid (BCA) Protein Assay Kit (Thermo Fisher Scientific, Rockford, IL, USA). Protein samples were separated using sodium dodecyl sulfate-polyacrylamide gel electrophoresis (SDS-PAGE) and transferred to polyvinylidene fluoride (PVDF) membranes (Cytiva, Marlborough, MA, USA) or nitrocellulose (NC)

membranes (GVS North America, Sanford, ME, USA). After transfer, PVDF membranes were blocked with 5% skim milk or bovine serum albumin in Tris-buffered saline with 0.1% Tween 20 (TBST) for 1 h at room temperature, followed by incubation with primary antibodies overnight at 4° C. The membranes were incubated with a secondary antibody conjugated with horseradish peroxidase (HRP) for 1 h at room temperature. Protein expression was detected using the ECL Western Blotting Substrate (Thermo Fisher Scientific). Western blots were imaged using an Alliance Q9 mini (UVITEC, Cambridge, England, UK).

For Phos-tag™ gel preparation, 25 μM Phos-tag™ acrylamide (Wako Pure Chemical Industries, Ltd., Osaka, Japan) containing $MnCl_2$ were added to 8% polyacrylamide separating gel solution according to the manufacturer's guidelines. Transfer of Phos-tag gel was performed with transfer buffer containing 0.1% SDS.

2.8. Cycloheximide chase assay

Cells were treated with DMSO or TA for 24 h and 40 μM of cycloheximide (CHX) was added at subsequent time intervals. The resulting cell lysates were subjected to western blotting analysis.

2.9. Proteasome inhibition analysis

Cells were treated with DMSO or TA as indicated and

simultaneously treated with epoxomicin or MG132. After 24 h, the cells were harvested and subjected to western blotting analysis as described above.

2.10. Ubiquitination assay

Cells were transfected using the above-mentioned plasmids for 6 - 12 h, followed by treatment with DMSO or TA with MG132. After 24 h, 500 μg of protein extracts were immunoprecipitated using Pierce™ Protein A/G Magnetic Beads (#88802; Thermo Fisher Scientific) or Protein A/G PLUS-Agarose (sc-2003; Santa Cruz Biotechnology) according to the manufacturer's protocol and subjected to western blotting analysis.

2.11. Nuclear-cytoplasmic protein fractionation

Protein fractionation was performed using an in-house cytoplasmic lysis buffer (10 mM HEPES, 2 mM $MgCl_2$, 1 mM EDTA, 1 mM EGTA, 10 mM KCl, 5 mM NaF, and 0.1 mM Na_3VO_4) and nuclear extraction buffer (25 mM HEPES, 500 mM NaCl, 10 mM NaF, 10% glycerol, 0.2% Nonidet P40, and 5 mM $MgCl_2$). The cells were seeded in a 100 mm cell culture dish before treatment. After treatment with DMSO or TA for 24 h, the cells were harvested using 400 μl of cytoplasmic lysis buffer. The cell lysates were incubated on ice for 10 min and 20 μl of 10% Nonidet P40 was added followed by incubation on ice for 3

min. The lysates were centrifuged at 12,000 xg at 4° C for 30 sec, and the supernatants (cytoplasmic protein) were collected. The centrifuged pellets were resuspended in 200 μl of nuclear extraction buffer and incubated on ice for 15 min. The pellets were centrifuged for 12,000 xg at 4° C for 10 min, and the supernatants (nuclear protein) were collected. Nuclear and cytoplasmic protein samples were subjected to western blotting analysis as described above.

2.12. Immunocytochemistry

Cells were seeded on a coverslip in a 6-well plate and transfected with empty vector, p2xflag-YAP, or p3xflag-TAZ using the PolyJet™ In Vitro DNA Transfection Reagent as previously described. After transfection, the cells were treated with DMSO or 50 μM of TA for 18 h. The cells were fixed with 4% paraformaldehyde for 15 min and washed twice with PBS. Flag antibody (1:5000) was added and incubated for 2 h at room temperature. The samples were washed twice with PBS and incubated with FITC-conjugated goat anti-mouse antibody (1:1000) for 1 h. DAPI (4′, 6-diamidino-2-phenylindole; 1 μg/mL, Roche, IN, USA) was used to stain the cell nucleus for 15 min. The coverslips were washed and mounted using a fluorescent mounting medium (#S3023; Dako North America, Carpinteria, CA, USA). The slides were visualized using an LSM900 confocal laser-scanning

microscope (CLSM) (ZEISS, Jena, Germany).

2.13. Statistical analysis

Student's t-test was used for comparisons between the two populations. All p-values were determined and statistical significance was considered at $*p < 0.05$, $**p < 0.01$, and $***p < 0.001$.

3. Results

3.1. *Tolfenamic acid inhibits cancer cell growth and YAP/TAZ target gene expression*

Tolfenamic acid (TA) is a well-known NSAID that inhibits tumorigenesis, including esophageal, pancreatic, and colorectal cancer. (Maen Abdelrahim et al., 2006; Papineni et al., 2009; Pathi, Li, & Safe, 2014). To determine the effects of TA on cancer cell proliferation, cell viability assays were performed using colorectal cancer cell lines (SW480, HCT116, LoVo) and a thyroid cancer cell line (BCPAP) (Figure 6). The results stated that dose-dependent TA administration inhibited cell growth in all the tested cells, which was in agreement with the previous reports from several groups demonstrating that TA affects cell growth in various cancer cell lines (Maen Abdelrahim et al., 2006; Papineni et al., 2009; Pathi et al., 2014). The Hippo pathway is closely related to cell viability and proliferation (Harvey, Zhang, & Thomas, 2013; Yu & Guan, 2013). The flag-tagged YAP or TAZ was transfected with the YAP/TAZ-responsive TEAD luciferase reporter (8xGTIIC) gene construct in HCT116 to determine the effect of TA on the Hippo pathway effectors. As shown in Figure 7, TA suppressed luciferase activity compared with DMSO control-treated samples. The results indicated that TA affects the YAP/TAZ-TEAD complex, resulting in the

suppression of TEAD responsiveness. Furthermore, quantitative reverse transcriptase-PCR (qRT-PCR) was performed to confirm the effect of TA on YAP/TAZ target gene expression. As shown in Figure 8A, the expression of NSAID-activated gene 1 (NAG-1), also known as growth/differentiation factor 15 (GDF15), increased after TA treatment, which was in agreement with previous studies (Kang et al., 2012; X. Wang, Baek, & Eling, 2013); however, the mRNA expression levels of CTGF decreased in the presence of TA. To determine whether the effect of TA is at the transcriptional or translational level, mRNA was extracted from HCT116 cells and qRT-PCR was performed (Figure 8B). Interestingly, no statistically significant change was observed in the mRNA expression of YAP, TAZ, or TEAD1, suggesting that TA affects YAP/TAZ expression at the translational or post-translational level. Therefore, TA inhibits the growth of cancer cells, which may be mediated through the inhibition of YAP/TAZ protein expression.

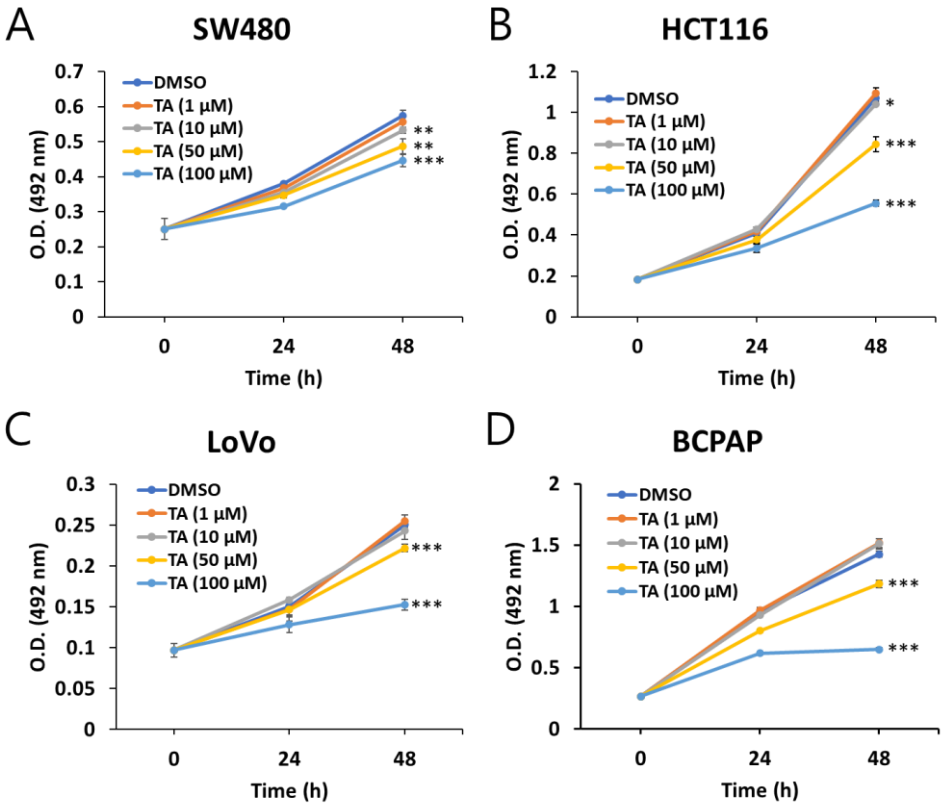

Figure 6. TA inhibits human cancer cell growth. (A–D) Cell viability assay of SW480 (A), HCT116 (B), LoVo (C), and BCPAP (D) cells treated with TA (n = 3). Error bars represent SD. *p < 0.05, **p < 0.01 and ***p < 0.001 by Student's t–test.

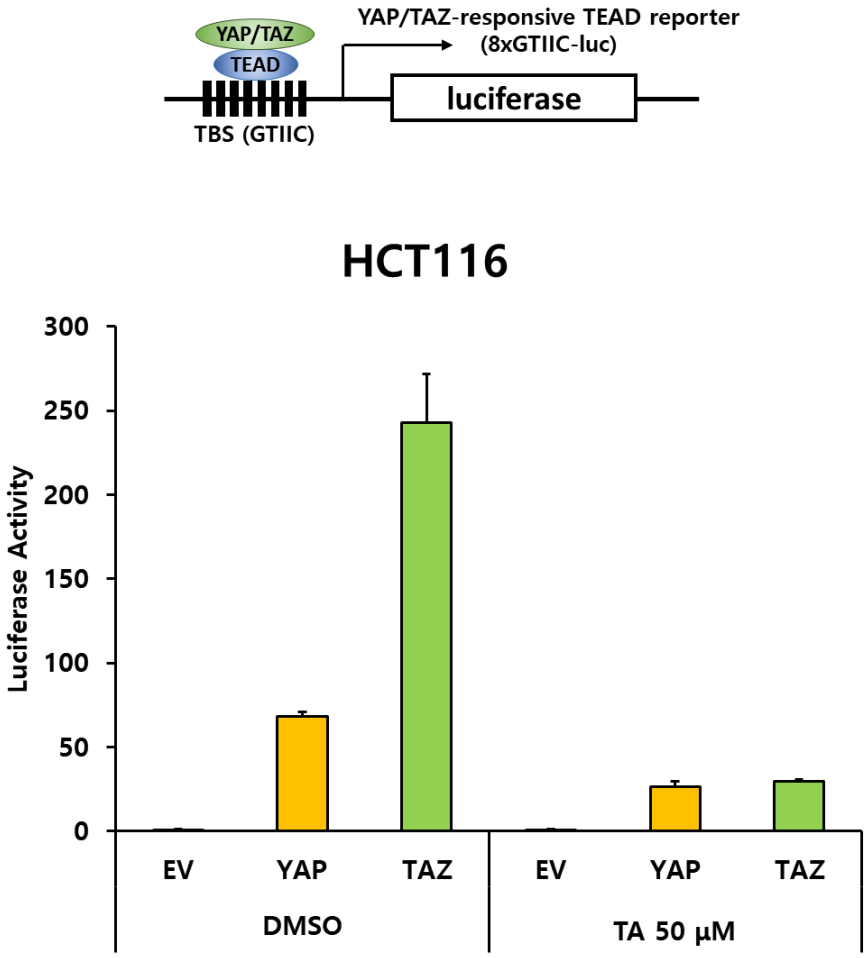

Figure 7. TA attenuates luciferase activity of YAP/TAZ-responsive TEAD-luciferase reporter. Luciferase assay of HCT116 cells transfected with the TEAD luciferase reporter (8xGTIIC-luc) and flag-YAP or flag-TAZ constructs, followed by TA treatment (n = 3). Error bars represent SD.

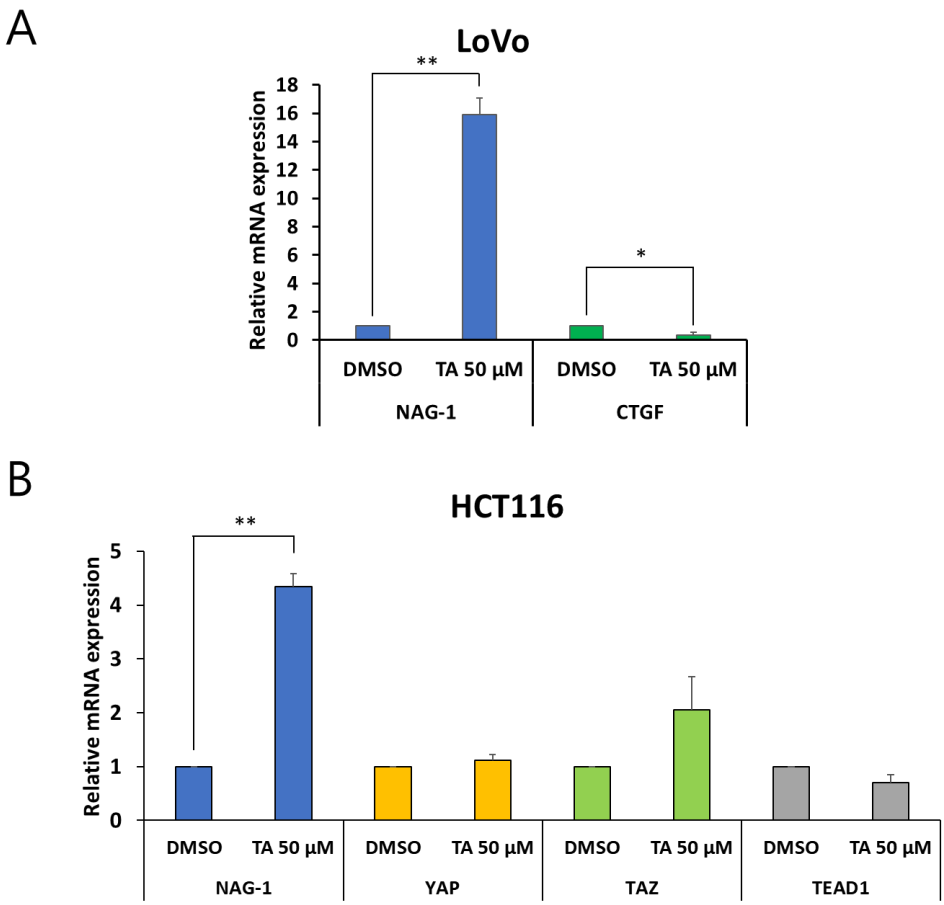

Figure 8. TA lowers YAP/TAZ target gene expression. (A, B) Quantitative reverse transcription PCR (qRT−PCR) results of LoVo (A) and HCT116 (B) cells treated with TA. Error bars represent SD. *p < 0.05, **p < 0.01 and ***p < 0.001 by Student's t−test.

3.2. *Tolfenamic acid attenuates YAP/TAZ protein level*

The effect of TA on the YAP/TAZ protein level was determined by western blotting analysis since there was no significant change in mRNA expression following TA treatment. Firstly, I treated various NSAIDs, including piroxicam, meloxicam, TA, sulindac sulfide, and celecoxib to SW480 cells and found that TAZ protein levels were reduced by TA, sulindac sulfide, or celecoxib, compared with the other NSAID-treated groups (Figure 9A). It was confirmed that NAG-1 protein levels were increased following TA treatment as previously reported (Kang et al., 2012; X. Wang et al., 2013). To determine whether the reduction of YAP/TAZ protein expression by TA occurs in a time- and dose-dependent manner, TA was treated to SW480 and LoVo colorectal cancer cells for various times and concentrations. As shown in Figure 9B-C, TA decreased YAP/TAZ protein level in a dose- and time-dependent manner. Notably, LoVo cells had less YAP protein compared with SW480 cells which were confirmed by the expression of YAP and TAZ. The flag-tagged YAP or TAZ also decreased at the protein level, indicating that TA affects YAP/TAZ protein expression (Figure 10A). To determine whether YAP/TAZ protein reduction by TA occurs in other cancer cells, TA was treated to U2OS osteosarcoma cells and BCPAP thyroid cancer cells. For both cell lines, a similar reduction of YAP/TAZ was

observed (Figure 10B). Human thyroid tissues from thyroid cancer patients were obtained and YAP/TAZ expression was examined in tumor tissues compared to adjacent normal tissues. The results indicated that the expression of YAP/TAZ in thyroid tumor tissue was higher compared with normal tissue, suggesting that YAP/TAZ protein was increased during thyroid tumorigenesis (Figure 11). Hence, the results signify that YAP/TAZ is highly expressed in tumor tissues and TA attenuates YAP/TAZ protein level.

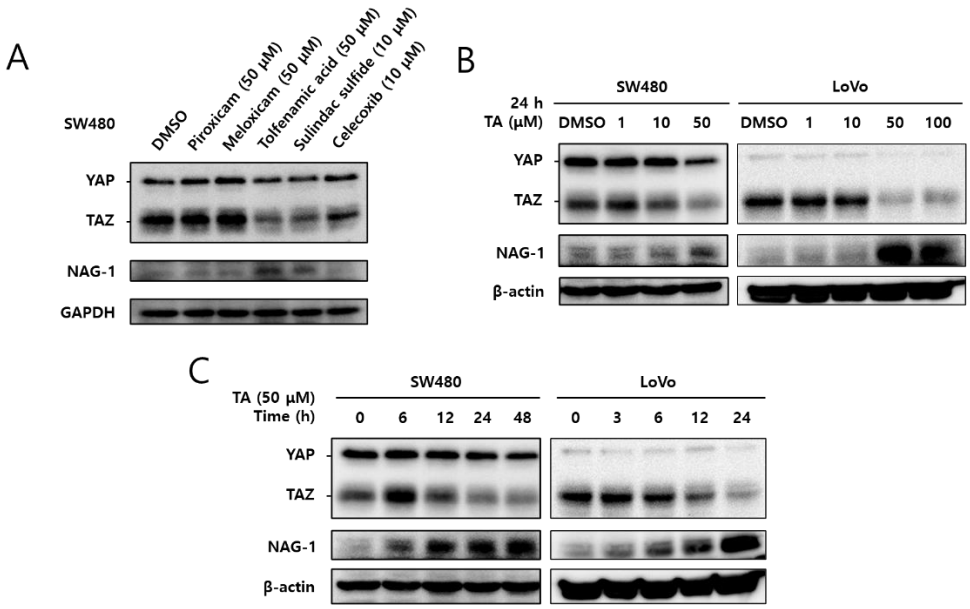

Figure 9. TA decreases YAP/TAZ protein level. (A) Immunoblotting of YAP/TAZ and NAG-1 in SW480 cells treated with various NSAIDs for 24 h. (B, C) Immunoblotting of YAP/TAZ and NAG-1 in SW480 and LoVo cells treated with TA in a dose-dependent (B) and time-dependent (C) manner.

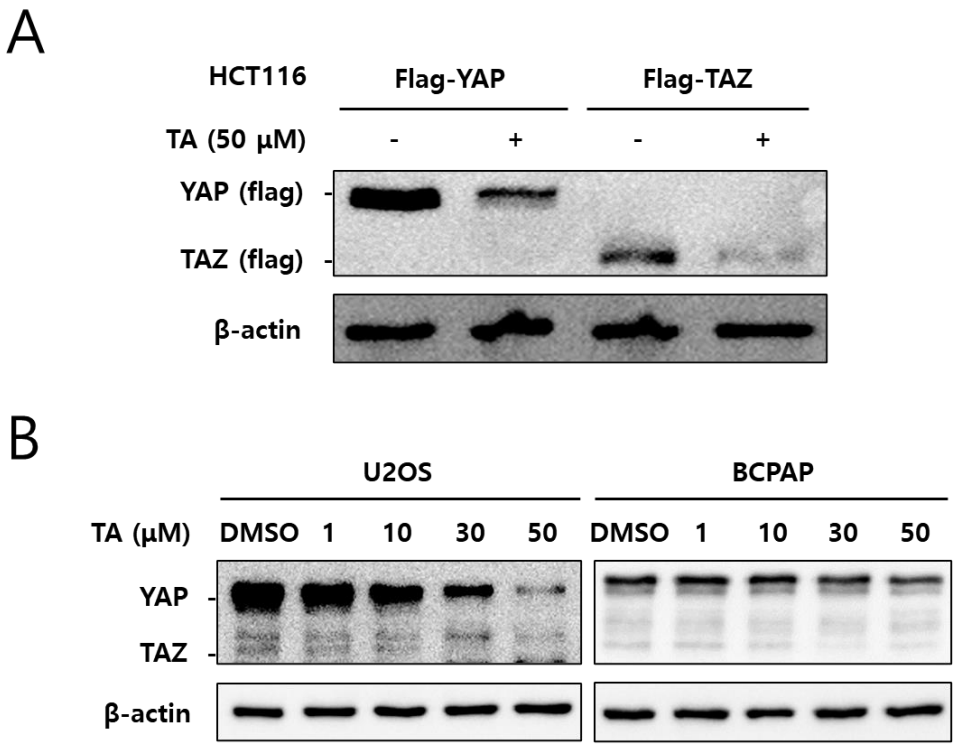

Figure 10. TA decreases YAP/TAZ protein level. (A) Immunoblotting of flag-tagged YAP and TAZ in HCT116 cells transfected with flag-YAP or flag-TAZ constructs and treated with TA for 24 h. (B) Immunoblotting of YAP/TAZ in U2OS and BCPAP cells treated with TA in a dose-dependent manner for 24 h.

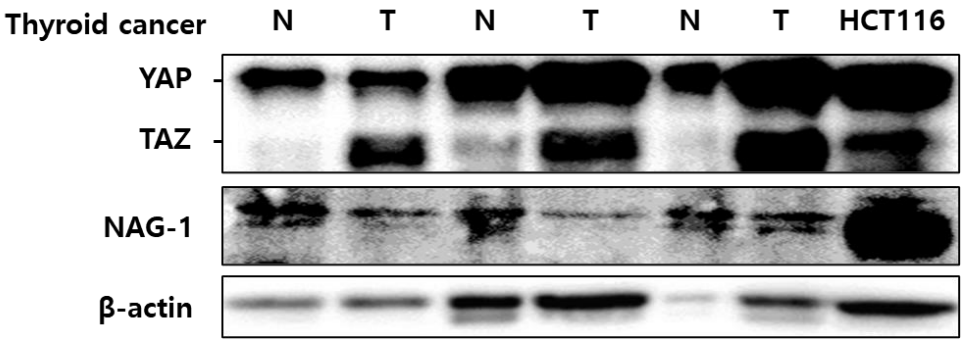

Figure 11. TAZ is highly expressed in human thyroid tumor tissues. Immunoblotting of YAP/TAZ and NAG−1 in normal (N) tissues (n = 3) and thyroid cancer (T) tissues (n = 3). HCT116 cell lysate was used as a positive control.

3.3. *Protein level change of NAG-1 and YAP/TAZ by Tolfenamic acid are independent*

Previous results indicated that NAG-1 may be involved in TA-mediated YAP/TAZ downregulation. To examine the negative correlation between NAG-1 and YAP/TAZ, I transfected NAG-1 siRNA to knockdown NAG-1 followed by TA treatment (Figure 12A). NAG-1 knockdown had no significant effect on YAP/TAZ reduction by TA. I overexpressed NAG-1 into the cells and YAP/TAZ expression was measured. As shown in Figure 12B, NAG-1 expression with various constructs, including wild-type, the uncleaved NAG-1 form (RXXR site mutant), cytoplasmic retention form (ΔNLS), and nuclear retention form (ΔNES) (Min et al., 2016), did not change YAP/TAZ expression. There is a previous report that YAP negatively controls NAG-1 expression at the transcriptional level (T. Wang et al., 2018). Therefore, I transfected TAZ siRNA to HCT116 and LoVo cells to knockdown TAZ, followed by TA treatment (Figure 12C-D). There was no remarkable change in the amount of NAG-1 protein between control and TAZ-KO cells. Hence, I assumed that the YAP/TAZ reduction and the NAG-1 induction occur through independent pathways.

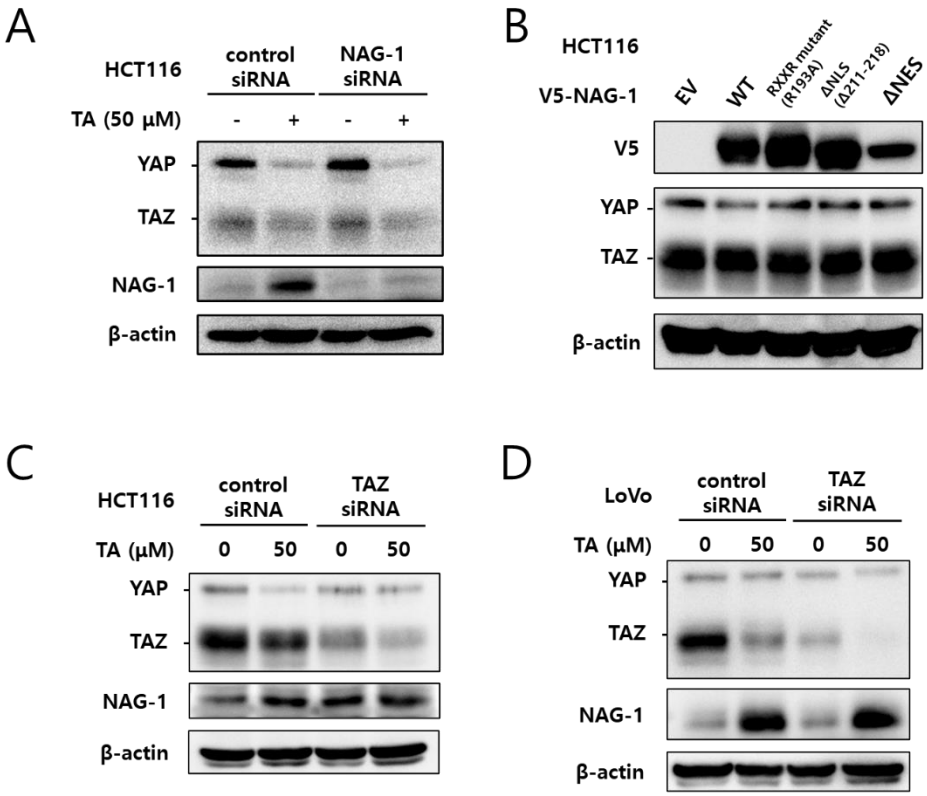

Figure 12. NAG-1 induction and YAP/TAZ reduction by TA occur in independent pathway. (A) Immunoblotting of YAP/TAZ and NAG-1 in HCT116 cells transfected with control or NAG-1 siRNA followed by TA treatment for 24 h. (B) Immunoblotting of a V5-tagged NAG-1 construct and YAP/TAZ in HCT116 cells. HCT116 cells were transfected with NAG-1 WT and mutant constructs (RXXR mutant, ΔNLS, and ΔNES). (C, D) Immunoblotting of YAP/TAZ and NAG-1. HCT116 (C) and LoVo (D) cells were transfected with control or TAZ siRNA and subsequently treated with TA for 24 h.

3.4. *YAP/TAZ degradation by Tolfenamic acid occurs through proteasomal degradation pathway*

TA treatment of cancer cells decreased YAP/TAZ protein levels without significant changes in YAP/TAZ mRNA expression (Figure 8B, 9-10). Therefore, I compared the YAP/TAZ reduction in DMSO- and TA-treated cells using a cycloheximide (CHX) chase assay. Both YAP and TAZ were degraded faster in the TA-treated group compared to the control, and the degradation rate of TAZ was higher than YAP in SW480 and LoVo cells (Figure 13A-B). This suggests that TA facilitates YAP/TAZ degradation at the post-translational level. It is well known that YAP/TAZ are ubiquitinated by $SCF^{\beta-TrCP}$ and degraded through the proteasomal degradation pathway once YAP and TAZ are phosphorylated (Piccolo et al., 2014; Yu & Guan, 2013). Therefore, I treated TA and the proteasome inhibitors, epoxomicin or MG132, to colorectal cancer cells and measured YAP/TAZ expression. YAP/TAZ were decreased in TA-treated cells when the proteasome inhibitors were absent, whereas YAP/TAZ were not decreased by TA in the presence of epoxomicin or MG132 (Figure 13C-E). These results suggested that TA degrades YAP/TAZ through the proteasomal degradation pathway.

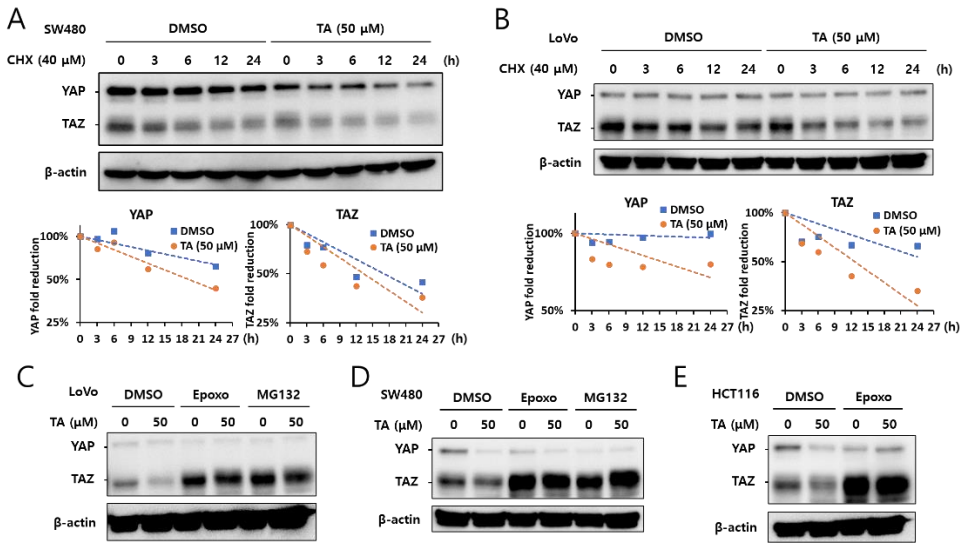

Figure 13. TA promotes YAP/TAZ degradation by proteasomal degradation pathway. (A, B) Cycloheximide chase assay of SW480 (A) and LoVo (B) cells following TA treatment. Cells were treated with TA for 24 h before CHX treatment. The protein levels of YAP and TAZ were measured using the ImageJ program and displayed graphically as shown in the figure. (C–E) Proteasome inhibition analysis of LoVo (C), SW480 (D), and HCT116 (E) cells. Cells were treated with TA and treated with epoxomicin (100 nM) and MG132 (10 μM). The protein levels of YAP/TAZ were measured by immunoblotting.

3.5. Tolfenamic acid increases YAP/TAZ phosphorylation

YAP/TAZ is phosphorylated by various kinases (He et al., 2016; Hicks-Berthet & Varelas, 2017). When phosphorylated, YAP/TAZ is retained in the cytoplasm by interaction with 14-3-3 protein or ubiquitinated and degraded through the proteasomal degradation pathway, depending on the site of phosphorylation (Piccolo et al., 2014; Yu & Guan, 2013). Therefore, I examined the changes caused by TA treatment on YAP/TAZ using a Phos-tag™ acrylamide gel that separates proteins according to their phosphorylation status. As shown in Figure 14A-B, the phosphorylated form of YAP/TAZ was increased in TA-treated cells compared with the control in all three cell lines. Of these, SW480 cells exhibited more phosphorylated YAP/TAZ compared with the other colorectal cancer cell lines. Since it has been known that the degradation of TAZ is mediated by the phosphorylation of a specific site; hence, I decided to find which phosphorylation sites on TAZ affected its degradation. I generated several mutant clones (S58/62A, S66A, S89/90A, S311/314A, and S66/89/311/314A) by mutating specific TAZ serine phosphorylation sites in them to alanine. The wild-type TAZ and mutant constructs were transfected into HCT116 cells followed by TA treatment to measure TAZ reduction. The phosphodegron sites (S58/62A and S311/314A) are known to be involved in TAZ degradation (He et al.,

2016; Hicks-Berthet & Varelas, 2017). As shown in Figure 14B, when these phosphodegron sites were mutated, the TAZ reduction rate was lower than wild-type TAZ. Meanwhile, the TAZ reduction rate was higher than wild-type TAZ when the site that binds to 14-3-3 protein (S66A and S89/90A) was mutated. These results indicated that TA increased the overall phosphorylation of YAP/TAZ and the phosphorylation of the TAZ phosphodegron site accelerated the TAZ protein degradation.

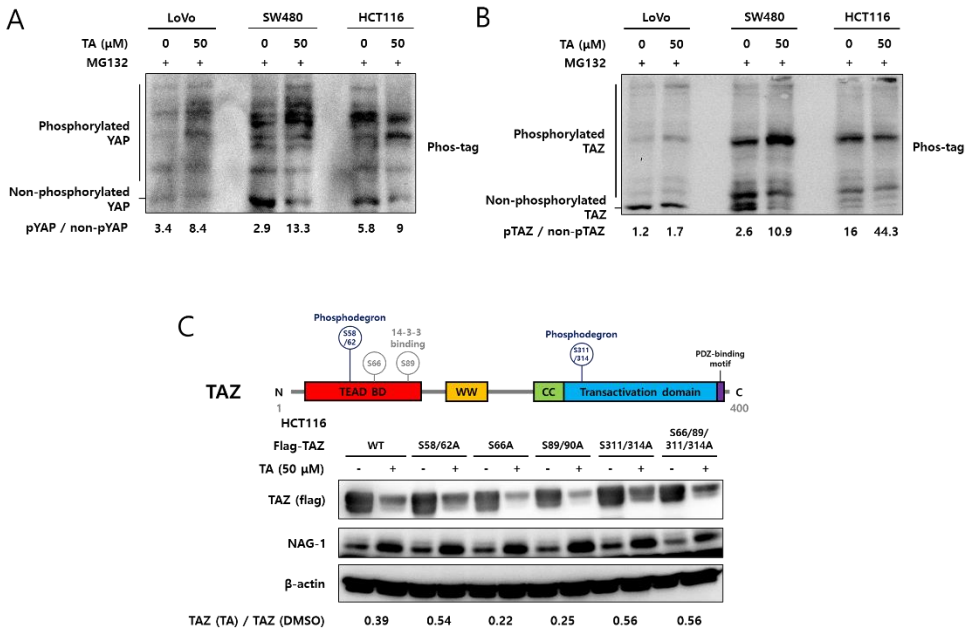

Figure 14. TA increases YAP/TAZ phosphorylation. (A, B) The phosphorylation status of YAP (A) and TAZ (B) was measured on a Phos-tag™ acrylamide gel for LoVo, SW480, and HCT116 cells after treatment with TA and MG132 (10 μM) for 24 h. The expression levels of phosphorylated YAP and TAZ were measured by ImageJ and the ratio of phosphorylated and non-phosphorylated YAP and TAZ is shown at the bottom of the immunoblot. (C) The structure of TAZ protein (upper panel) and immunoblotting of flag-tagged TAZ and NAG-1 in HCT116 cells (lower panel) are shown. HCT116 cells were transfected with flag-TAZ WT and mutant constructs (TAZ S58/62A, S66A, S89/90A, and S66/89/311/314A) and subsequently

treated with TA for 24 h. The protein levels of TAZ were measured by ImageJ and the ratio of TAZ from control and TA−treated cells is shown at the bottom of the immunoblot.

3.6. Tolfenamic acid promotes ubiquitination of YAP/TAZ

It is well known that YAP/TAZ gets bound by 14-3-3 protein after phosphorylation at specific sites and localized in the cytoplasm (Piccolo et al., 2014; Yu & Guan, 2013). I performed western blotting analysis after treating LoVo and SW480 cells with TA to determine the change in protein level of 14-3-3. As shown in Figure 15A, no visible change was observed in the protein amount of pan 14-3-3. However, protein level of exogenous 14-3-3β was decreased in TA-treated cells, which was observed in both HCT116 and LoVo cells (Figure 15B). These results show that TA may affect the protein level of 14-3-3 isotypes, but not total protein level of pan 14-3-3. TA increased YAP/TAZ phosphorylation and decreased its levels through the proteasomal degradation pathway; hence, I transfected flag-YAP and HA-ubiquitin into HCT116 cells followed by treatment with TA and performed ubiquitination assay. In the TA-treated cells, the ubiquitination of YAP was increased compared with the control (Figure 15C, lane 4, 5). It is also found that YAP was bound with 14-3-3β (lane 6, 7). Similarly, the increased ubiquitination of TAZ by TA was observed in SW480 cells transfected with flag-TAZ (Figure 15D); These results suggest that TA increases YAP/TAZ ubiquitination, thereby enhancing YAP/TAZ degradation.

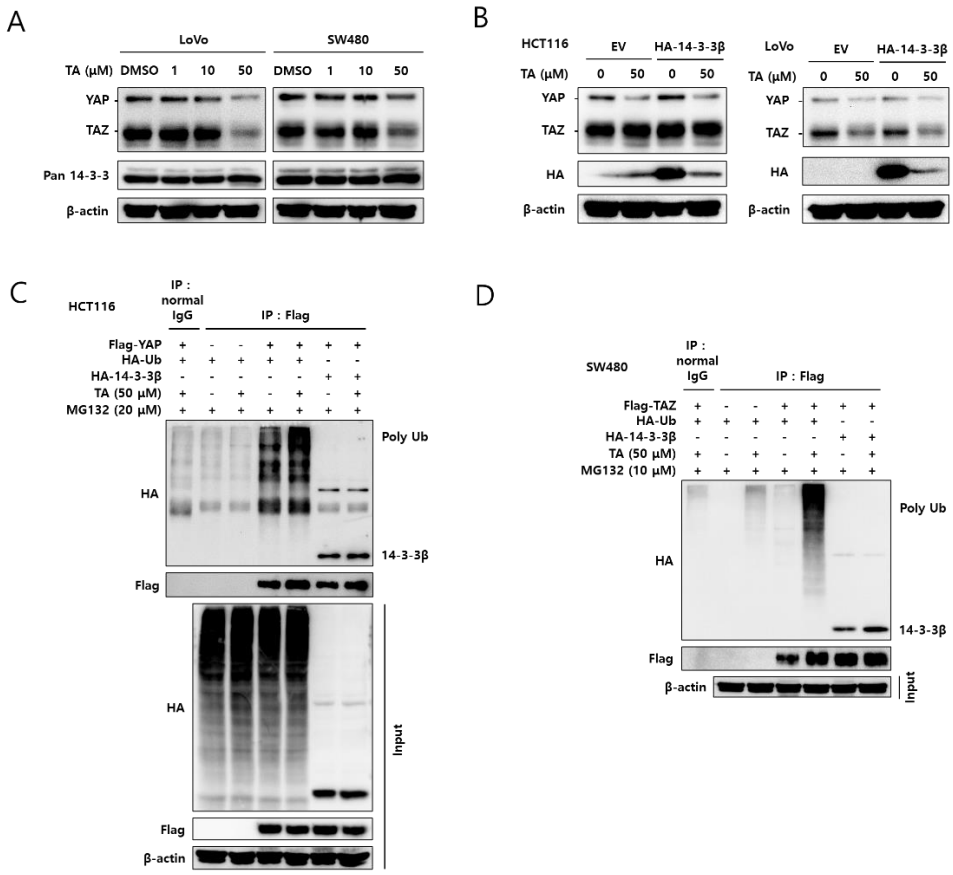

Figure 15. TA increases YAP/TAZ ubiquitination. (A) Immunoblotting of YAP/TAZ and pan 14-3-3 in LoVo and SW480 cells treated with TA in a dose-dependent manner for 24 h. (B) Immunoblotting of YAP/TAZ and HA-tagged 14-3-3β in HCT116 and LoVo cells transfected with HA-14-3-3β, followed by TA treatment for 24 h. (C) Co-immunoprecipitation in HCT116 cells transfected with flag-YAP, HA-Ub, and HA-14-3-3β and subsequent treatment with TA and MG132. Whole-cell lysates were immunoprecipitated with flag-YAP and immunoblotted for HA-Ub,

HA−14−3−3β, and flag−YAP. (D) Co−immunoprecipitation in SW480 cells transfected with flag−TAZ, HA−Ub, and HA−14−3−3β and subsequent treatment with TA and MG132. Whole−cell lysates were immunoprecipitated with flag−TAZ and immunoblotted for HA−Ub, HA−14−3−3β, and flag−TAZ.

3.7. Cytoplasmic localization of YAP/TAZ is increased by Tolfenamic acid treatment

To further investigate the cellular localization of YAP/TAZ affected by TA, nuclear/cytoplasmic fractionation was performed following TA treatment in LoVo, SW480, and HCT116 cells. As shown in Figure 16A, nuclear YAP/TAZ (lane 4) was lower than control (lane 2) in TA-treated cells, suggesting that the nuclear localization of YAP/TAZ was decreased by phosphorylation and cytoplasmic retention. Meanwhile, cytoplasmic YAP/TAZ (lane 3) in TA-treated cells was also lower than in the control (lane 1), which suggests that the degradation of YAP/TAZ occurred in the cytoplasm and nucleus. To confirm the western blotting results and verify the cellular localization of YAP/TAZ, immunocytochemistry was performed in HCT116 cells. As shown in Figure 16B, YAP and TAZ exhibited increased localization in the cytoplasm compared to the nucleus in TA-treated cells relative to the control.

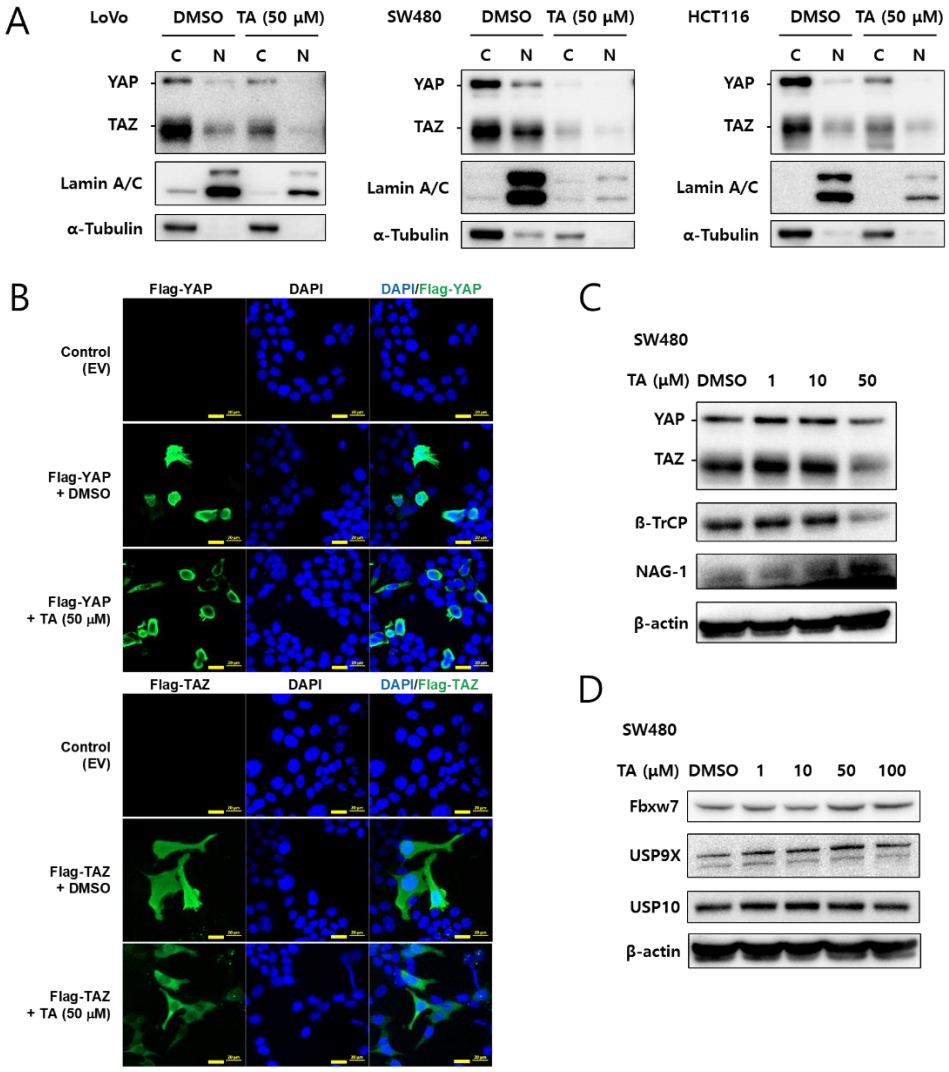

Figure 16. TA increases cytoplasmic localization of YAP/TAZ. (A) Nuclear-cytoplasmic fractionation in LoVo, SW480, and HCT116 cells treated with TA for 24 h. YAP/TAZ expression was measured by immunoblotting. (B) Immunocytochemistry of HCT116 cells transfected with flag-YAP or flag-TAZ and treated with TA for 24 h. Nuclei are shown in blue (DAPI) and flag-tagged YAP and TAZ

are shown in green (FITC). Scale bars = 20 μm. (C, D) Immunoblotting for YAP/TAZ, β−TrCP, NAG−1 (C), Fbxw7, USP9X, and USP10 (D) in SW480 cells treated with TA in a dose−dependent manner for 24 h.

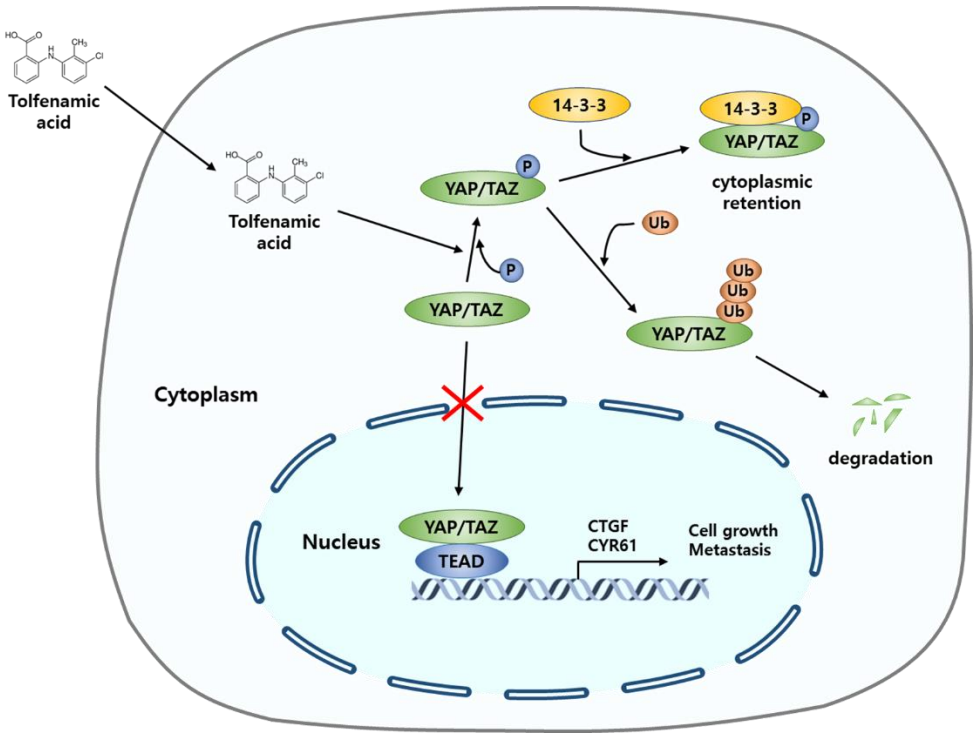

Figure 17. Schematic diagram of YAP/TAZ protein localization and degradation affected by TA treatment.

4. Discussion

The YAP/TAZ proteins are downstream modulators of the Hippo signaling pathway. They regulate many genes that are involved in metastasis and function as oncogenic proteins (Piccolo et al., 2014; Yu & Guan, 2013). YAP/TAZ is regulated by phosphorylation and other post-translational modifications induced by cell stress through Hippo signaling-dependent and -independent mechanisms (He et al., 2016; Hicks-Berthet & Varelas, 2017). YAP/TAZ is also involved in amino acid metabolism (Koo & Guan, 2018) and glucose metabolism (Enzo et al., 2015), indicating that they play a role in cancer metabolism. Because YAP/TAZ controls various cellular functions necessary for metastasis, including cell migration, invasion, and epithelial-mesenchymal transition, it is important to investigate how YAP/TAZ activity is inhibited in cancer cells fpr the potential therapeutic targets.

Evidence from several sources indicates that using NSAIDs on a long-term basis lowers the risk of developing cancer. Epidemiological and animal studies have revealed a negative correlation between the use of NSAIDs and the prevalence of various cancers (Wong, 2019). Cyclooxygenase-dependent and -independent pathways are involved in the anti-cancer activity of NSAIDs (Liggett, Zhang, Eling, & Baek, 2014). In particular, TA was

reported to exhibit anti-cancer activity through Sp1 (Maen Abdelrahim et al., 2006), NAG-1 (Won Chang et al., 2013), ATF3 (Lee et al., 2010), and the ESE-1/EGR-1 pathways (Lee et al., 2008) in colorectal cancer cells; however, other molecular mechanisms may be involved in the TA effect on anti-cancer activity. Among the other NSAIDs, the advantage of TA in exhibiting anti-cancer activity has been reported (Maen Abdelrahim et al., 2006; Lee et al., 2008). Interestingly, I found that TA was the most effective NSAID for YAP/TAZ degradation compared with the other tested NSAIDs (Figure 9A). These results indicated that TA exerts higher anti-cancer activity than other NSAIDs.

Several tyrosine kinases control YAP/TAZ activity by phosphorylation and enhance metastasis (Kedan et al., 2018). Thus, phosphorylation/dephosphorylation of YAP/TAZ may be an important event in controlling its stability since phosphorylated YAP/TAZ is either degraded by ubiquitination or retained by 14-3-3 protein in the cytoplasm. TA affects the hyper-phosphorylation of YAP/TAZ (Figure 14A-B); hence, I subsequently determined a phosphorylation map of TAZ to elucidate which phosphorylation site plays a role in TA-induced TAZ degradation. There was no apparent specific phosphorylation site involved in the TA effect; however, at least I found that S58/62 and S311/S314 mutations resulted in less TAZ degradation compared with the wild-type control. Interestingly,

these sites are known as phosphodegron sites (Figure 14C), which are the targets of ubiquitination recognizing and recruiting E3 ligase (He et al., 2016; Hicks-Berthet & Varelas, 2017).

Several known E3 ligases promote TAZ degradation, including β-TrCP and Fbxw7, and deubiquitinases, such as USP9X and USP10, inhibit TAZ degradation. TAZ protein stability is controlled by a phosphodegron recognized by the SCF/CRL1$^{\beta-\mathrm{TrCP}}$ E3 ligase (Liu et al., 2010). USP9X is a deubiquitinase that controls Fbxw7 in colon cancer (Khan et al., 2018), whereas USP10 stabilizes YAP/TAZ in hepatocellular carcinoma (Zhu et al., 2020). I investigated protein expression in the presence of TA and found that most of these proteins were unaffected by TA in terms of protein expression (Figure 16C-D). Unexpectedly, β-TrCP expression was downregulated in the presence of TA. A detailed study may be required to explain why β-TrCP was downregulated by TA; however, our results indicate that TAZ degradation by TA is not primarily affected by YAP/TAZ-E3 ligase. Further experiments are required to elucidate the detailed mechanism by which TA affects YAP/TAZ degradation concerning miRNA levels and other post-translational modifications.

To determine whether TA affects the ubiquitination pathway, cells were transfected with flag-YAP or flag-TAZ and an HA-Ub plasmid. As shown in Figure 15, TA increased the phosphorylation of YAP and

TAZ protein, followed by increased ubiquitination. The 14-3-3 proteins are cytoplasmic proteins that play an important role in the regulation of signaling pathways, cell proliferation, apoptosis, differentiation, and survival (Freeman & Morrison, 2011). They perform these functions by binding and modulating the activity of key regulatory proteins, such as TAZ and YAP. For example, 14-3-3β was reported to exhibit oncogenic potential and its increased expression has been observed in multiple types of cancer (Gong et al., 2013; Tang, Lv, Sun, Han, & Zhou, 2016; Tseng et al., 2011). Although TA did not affect the pan-14-3-3 proteins, TA decreased 14-3-3β expression (Figure 15B), which indicated other activity of TA in anti-tumorigenesis. Thus, TA not only affects YAP/TAZ but also 14-3-3β expression, thereby enhancing its anti-tumorigenic effect. Decreasing 14-3-3β expression by TA may be another benefit for treating cancer patients.

NAG-1 belongs to the transforming growth factor-β protein superfamily. It is a moonlighting protein that controls its function depending on its intercellular location (X. Wang et al., 2013). Additionally, TA increases NAG-1 expression in colorectal cancer cells and head and neck cancer (Kang et al., 2012). To identify the molecular mechanism through which TA suppresses YAP/TAZ expression, I examined the role of NAG-1. Although there is a strong correlation between NAG-1 expression and TAZ downregulation, I

could not find any direct evidence proving that NAG-1 mediates TA-induced TAZ downregulation (Figure 12). Thus, NAG-1 induction by TA represents TA-mediated anti-cancer mechanism in colorectal cancer cells.

In this study, I elucidated a novel function of TA in YAP/TAZ regulation. Our results provide a more comprehensive understanding of the anti-cancer effects of TA (Figure 17). Although further research is required to elucidate the precise molecular mechanism of TA in YAP/TAZ degradation, our data strongly support the role of the Hippo pathway in regulating the anti-tumorigenic activity of TA.

5. References

Abdelrahim, M., Baker, C. H., Abbruzzese, J. L., & Safe, S. (2006). Tolfenamic acid and pancreatic cancer growth, angiogenesis, and Sp protein degradation. *J Natl Cancer Inst, 98*(12), 855-868.

Abdelrahim, M., Baker, C. H., Abbruzzese, J. L., Sheikh-Hamad, D., Liu, S., Cho, S. D., et al. (2007). Regulation of vascular endothelial growth factor receptor-1 expression by specificity proteins 1, 3, and 4 in pancreatic cancer cells. *Cancer Res 67(7)*, 3286-3294. .

Ahmad, F. B., & Anderson, R. N. (2021). The Leading Causes of Death in the US for 2020. *JAMA, 325*(18), 1829-1830. doi:10.1001/jama.2021.5469

Baek, S. J., Kim, K.-S., Nixon, J. B., Wilson, L. C., & Eling, T. E. (2001). Cyclooxygenase inhibitors regulate the expression of a TGF-β superfamily member that has proapoptotic and antitumorigenic activities. *Mol Pharmacol, 59*(4), 901-908.

Basu, S., Totty, N. F., Irwin, M. S., Sudol, M., & Downward, J. (2003). Akt phosphorylates the Yes-associated protein, YAP, to induce interaction with 14-3-3 and attenuation of p73-mediated apoptosis. *Mol Cell, 11*(1), 11-23. Retrieved from https://www.ncbi.nlm.nih.gov/pubmed/12535517

Calses, P. C., Crawford, J. J., Lill, J. R., & Dey, A. (2019). Hippo pathway in cancer: aberrant regulation and therapeutic

opportunities. *Trends in cancer, 5*(5), 297-307.

Chen, Y.-A., Lu, C.-Y., Cheng, T.-Y., Pan, S.-H., Chen, H.-F., & Chang, N.-S. (2019). WW domain-containing proteins YAP and TAZ in the hippo pathway as key regulators in stemness maintenance, tissue homeostasis, and tumorigenesis. *Front Oncol, 9*, 60.

Enzo, E., Santinon, G., Pocaterra, A., Aragona, M., Bresolin, S., Forcato, M., et al. (2015). Aerobic glycolysis tunes YAP/TAZ transcriptional activity. *EMBO J, 34*(10), 1349-1370.

Freeman, A. K., & Morrison, D. K. (2011). *14-3-3 Proteins: diverse functions in cell proliferation and cancer progression.* Paper presented at the Semin Cell Dev Biol.

Gong, F., Wang, G., Ye, J., Li, T., Bai, H., & Wang, W. (2013). 14-3-3β regulates the proliferation of glioma cells through the GSK3β/β-catenin signaling pathway. *Oncol Rep, 30*(6), 2976-2982.

Hansen, P. E. (1994). Tolfenamic acid in acute and prophylactic treatment of migraine: a review. *Pharmacol Toxicol, 75 Suppl 2*, 81-82. Retrieved from http://www.ncbi.nlm.nih.gov/pubmed/7816790

Hansen, S. H., & Pedersen, S. B. (1986). Assay of tolfenamic acid and its metabolites by liquid chromatography on dynamically modified silica: Application in pharmacokinetics. *J Pharm Biomed Anal, 4*(1), 69-82. Retrieved from

http://www.ncbi.nlm.nih.gov/entrez/query.fcgi?cmd=Retrieve&db=PubMed&dopt=Citation&list_uids=16867632

Harvey, K. F., Zhang, X., & Thomas, D. M. (2013). The Hippo pathway and human cancer. *Nat Rev Cancer, 13*(4), 246-257.

He, M., Zhou, Z., Shah, A. A., Hong, Y., Chen, Q., & Wan, Y. (2016). New insights into posttranslational modifications of Hippo pathway in carcinogenesis and therapeutics. *Cell Div, 11*(1), 1-10.

Hicks-Berthet, J., & Varelas, X. (2017). Integrin-FAK-CDC42-PP1A signaling gnaws at YAP/TAZ activity to control incisor stem cells. *Bioessays, 39*(10), 1700116.

Huang, W., Lv, X., Liu, C., Zha, Z., Zhang, H., Jiang, Y., et al. (2012). The N-terminal phosphodegron targets TAZ/WWTR1 protein for SCFbeta-TrCP-dependent degradation in response to phosphatidylinositol 3-kinase inhibition. *J Biol Chem, 287*(31), 26245-26253. doi:10.1074/jbc.M112.382036

Juan, W. C., & Hong, W. (2016). Targeting the Hippo Signaling Pathway for Tissue Regeneration and Cancer Therapy. *Genes (Basel), 7*(9). doi:10.3390/genes7090055

Kang, S. U., Shin, Y. S., Hwang, H. S., Baek, S. J., Lee, S.-H., & Kim, C.-H. (2012). Tolfenamic acid induces apoptosis and growth inhibition in head and neck cancer: involvement of NAG-1 expression. *PLoS One, 7*(4), e34988.

Kedan, A., Verma, N., Saroha, A., Shreberk-Shaked, M., Müller, A.-

K., Nair, N. U., et al. (2018). PYK2 negatively regulates the Hippo pathway in TNBC by stabilizing TAZ protein. *Cell Death Dis, 9*(10), 985. doi:10.1038/s41419-018-1005-z

Khan, O. M., Carvalho, J., Spencer-Dene, B., Mitter, R., Frith, D., Snijders, A. P., et al. (2018). The deubiquitinase USP9X regulates FBW7 stability and suppresses colorectal cancer. *J Clin Invest, 128*(4), 1326-1337.

Kim, Y., Kim, W., Song, Y., Kim, J. R., Cho, K., Moon, H., et al. (2017). Deubiquitinase YOD1 potentiates YAP/TAZ activities through enhancing ITCH stability. *Proc Natl Acad Sci U S A, 114*(18), 4691-4696. doi:10.1073/pnas.1620306114

Koo, J. H., & Guan, K.-L. (2018). Interplay between YAP/TAZ and Metabolism. *Cell Metab, 28*(2), 196-206.

Lee, S. H., Bahn, J. H., Choi, C. K., Whitlock, N. C., English, A. E., Safe, S., et al. (2008). ESE-1/EGR-1 pathway plays a role in tolfenamic acid-induced apoptosis in colorectal cancer cells. *Mol Cancer Ther, 7*(12), 3739-3750. doi:10.1158/1535-7163.MCT-08-0548

Lee, S. H., Bahn, J. H., Whitlock, N. C., & Baek, S. J. (2010). Activating transcription factor 2 (ATF2) controls tolfenamic acid-induced ATF3 expression via MAP kinase pathways. *Oncogene, 29*(37), 5182-5192. doi:10.1038/onc.2010.251

Liggett, J. L., Zhang, X., Eling, T. E., & Baek, S. J. (2014). Anti-

tumor activity of non-steroidal anti-inflammatory drugs: cyclooxygenase-independent targets. *Cancer Lett, 346*(2), 217-224. doi:10.1016/j.canlet.2014.01.021

Liu, C.-Y., Zha, Z.-Y., Zhou, X., Zhang, H., Huang, W., Zhao, D., et al. (2010). The hippo tumor pathway promotes TAZ degradation by phosphorylating a phosphodegron and recruiting the SCF β-TrCP E3 ligase. *J Biol Chem, 285*(48), 37159-37169.

Min, K., Liggett, J., Silva, G., Wu, W., Wang, R., Shen, R., et al. (2016). NAG-1/GDF15 accumulates in the nucleus and modulates transcriptional regulation of the Smad pathway. *Oncogene, 35*(3), 377-388.

Mo, J. S., Meng, Z., Kim, Y. C., Park, H. W., Hansen, C. G., Kim, S., et al. (2015). Cellular energy stress induces AMPK-mediated regulation of YAP and the Hippo pathway. *Nat Cell Biol, 17*(4), 500-510. doi:10.1038/ncb3111

Papineni, S., Chintharlapalli, S., Abdelrahim, M., Lee, S.-o., Burghardt, R., Abudayyeh, A., et al. (2009). Tolfenamic acid inhibits esophageal cancer through repression of specificity proteins and c-Met. *Carcinogenesis, 30*(7), 1193-1201.

Pathi, S., Li, X., & Safe, S. (2014). Tolfenamic acid inhibits colon cancer cell and tumor growth and induces degradation of specificity protein (Sp) transcription factors. *Mol Carcinog, 53*(S1), E53-E61.

Piccolo, S., Cordenonsi, M., & Dupont, S. (2013). Molecular pathways: YAP and TAZ take center stage in organ growth and tumorigenesis. *Clin Cancer Res, 19*(18), 4925-4930. doi:10.1158/1078-0432.CCR-12-3172

Piccolo, S., Dupont, S., & Cordenonsi, M. (2014). The Biology of Yap/Taz: Hippo Signaling and Beyond. *Physiol Rev, 94*(4), 1287-1312. doi:10.1152/physrev.00005.2014

Piersma, B., Bank, R. A., & Boersema, M. (2015). Signaling in Fibrosis: TGF-beta, WNT, and YAP/TAZ Converge. *Front Med (Lausanne), 2*, 59. doi:10.3389/fmed.2015.00059

Sebio, A., & Lenz, H. J. (2015). Molecular Pathways: Hippo Signaling, a Critical Tumor Suppressor. *Clin Cancer Res, 21*(22), 5002-5007. doi:10.1158/1078-0432.CCR-15-0411

Song, J., Wang, T., Chi, X., Wei, X., Xu, S., Yu, M., et al. (2019). Kindlin-2 Inhibits the Hippo Signaling Pathway by Promoting Degradation of MOB1. *Cell Rep, 29*(11), 3664-3677 e3665. doi:10.1016/j.celrep.2019.11.035

Tang, Y., Lv, P., Sun, Z., Han, L., & Zhou, W. (2016). 14-3-3β promotes migration and invasion of human hepatocellular carcinoma cells by modulating expression of MMP2 and MMP9 through PI3K/Akt/NF-κB pathway. *PLoS One, 11*(1), e0146070.

Tseng, C. W., Yang, J. C., Chen, C. N., Huang, H. C., Chuang, K. N., Lin, C. C., et al. (2011). Identification of 14-3-3β in human gastric

cancer cells and its potency as a diagnostic and prognostic biomarker. *Proteomics, 11*(12), 2423-2439.

Varelas, X. (2014). The Hippo pathway effectors TAZ and YAP in development, homeostasis and disease. *Development, 141*(8), 1614-1626. doi:10.1242/dev.102376

Wang, T., Mao, B., Cheng, C., Zou, Z., Gao, J., Yang, Y., et al. (2018). YAP promotes breast cancer metastasis by repressing growth differentiation factor-15. *Biochim Biophys Acta Mol Basis Dis, 1864*(5), 1744-1753.

Wang, X., Baek, S. J., & Eling, T. E. (2013). The diverse roles of nonsteroidal anti-inflammatory drug activated gene (NAG-1/GDF15) in cancer. *Biochem Pharmacol, 85*(5), 597-606.

Won Chang, J., Kang, S. U., Choi, J. W., Shin, Y. S., Baek, S. J., Lee, S. H., et al. (2013). Tolfenamic Acid Induces Apoptosis and Growth Inhibition in Anaplastic Thyroid Cancer: Involvement of NAG-1 Expression and Intracellular ROS Generation. *Free Radic Biol Med*. doi:10.1016/j.freeradbiomed.2013.10.818

Wong, R. S. Y. (2019). Role of Nonsteroidal Anti-Inflammatory Drugs (NSAIDs) in Cancer Prevention and Cancer Promotion. *Adv Pharmacol Sci, 2019*, 3418975. doi:10.1155/2019/3418975

Yu, F.-X., & Guan, K.-L. (2013). The Hippo pathway: regulators and regulations. *Genes Dev, 27*(4), 355-371.

Yu, F.-X., Zhao, B., & Guan, K.-L. (2015). Hippo pathway in organ

size control, tissue homeostasis, and cancer. *Cell, 163*(4), 811–828.

Zanconato, F., Cordenonsi, M., & Piccolo, S. (2016). YAP/TAZ at the Roots of Cancer. *Cancer Cell, 29*(6), 783–803. doi:10.1016/j.ccell.2016.05.005

Zhang, B., Gong, A., Shi, H., Bie, Q., Liang, Z., Wu, P., et al. (2017). Identification of a novel YAP–14–3–3zeta negative feedback loop in gastric cancer. *Oncotarget, 8*(42), 71894–71910. doi:10.18632/oncotarget.18011

Zhang, X., Min, K. W., Liggett, J., & Baek, S. J. (2013). Disruption of the transforming growth factor–beta pathway by tolfenamic acid via the ERK MAP kinase pathway. *Carcinogenesis*. doi:10.1093/carcin/bgt250

Zhu, H., Yan, F., Yuan, T., Qian, M., Zhou, T., Dai, X., et al. (2020). USP10 promotes proliferation of hepatocellular carcinoma by deubiquitinating and stabilizing YAP/TAZ. *Cancer Res, 80*(11), 2204–2216.

국문 초록

톨페남산(Tolfenamic acid)에 의한 YAP 및 TAZ 단백질 분해와 암세포 성장 억제 효과

서울대학교 대학원

수의학과 수의생명과학전공

김 일 주

지도교수 백 승 준

Hippo 신호전달경로(Hippo pathway)는 세포 증식과 암 전이에 중요한 역할을 하는 신호 경로이다. 암을 비롯한 여러 질병은 이 경로의 부적절한 조절과 관련이 있다고 알려져 있다. Hippo 경로의 주요 효과인자(effector)인 YAP 및 TAZ 단백질의 과발현은 종양 조직에서 암세포의 증식, 생존 및 전이를 가속화한다. 톨페남산(Tolfenamic acid)은 다양한 유형의 암에 대해 항암 작용을 나타내는 비스테로이드성 항염증제(NSAID)이다. 본 연구에서는 톨페남산이 암세포에서 YAP과 TAZ 단

백질량을 감소시킨다는 것을 관찰하였다. 톨페남산은 YAP 및 TAZ의 인산화(phosphorylation)를 증가시켜 세포질과 핵에서 YAP과 TAZ의 분해를 유도한다. 특히 톨페남산은 TAZ 단백질의 포스포데그론(phosphodegron) 부위에 주로 영향을 미쳐 TAZ가 유비퀴틴화(ubiquitination) 경로로 들어가도록 유도한다. 본 연구에서 NAG-1 및 여러 YAP/TAZ E3 연결효소 등 기존에 YAP/TAZ 발현에 영향을 준다고 알려진 단백질들은 톨페남산 매개 YAP/TAZ 발현 감소에 관여하지 않는 것으로 밝혀졌다. 요약하면, 본 연구 결과는 톨페남산이 YAP과 TAZ 발현량을 감소시키고 TAZ 단백질의 포스포데그론 부위에 영향을 미치며, 향후 종양 치료에 톨페남산을 활용할 수 있는 새로운 가능성을 보여준다.

주요어: Hippo 신호전달경로, YAP, TAZ, NAG-1, 14-3-3, 항암 효과

학 번: 2021-24740

Acknowledgements

First and foremost, I wish to express my sincere appreciation to my advisor, Prof. Seung Joon Baek, for his patience, guidance, and support. I have benefited greatly from his wealth of knowledge and meticulous editing. I am extremely grateful that he took me on as a student and continued to have faith in me over the years. Without his persistent help, the goal of this project would not have been realized.

I wish to show my gratitude to my committee members, Prof. Je-Yoel Cho and Prof. Soyeong Lee. Their encouraging words and thoughtful, detailed feedback have been very important to me.

I would like to add that I am grateful to the laboratory members, Jaehak Lee, Yukyung Hong, Pattawika Lertpatipanpong, Kanokkan Boonruang, who so generously took time out of their schedules to participate in my research and make this project possible.

Last but not least, I wish to acknowledge the support and great love of my parents for their continuous love and support. They have always stood behind me.